

Chapter 5

Evaluation of a PV-driven innovative solar dryer with and without sensible heat storage for *Garcinia pedunculata*: An investigation on exergy and environmental aspects

Traditionally, the performance of a dryer is evaluated using the first law of thermodynamics, which offers a quantitative measure of energy as discussed in Chapter 4 but excludes details such as the magnitude and location of irreversible losses in the system [97]. Exergy studies overcome this barrier and better represent the improvement potential of the drying system. Moreover, the environmental study of solar dryers provides a great deal of information regarding CO₂ emissions [4,115]. This chapter provides the information on the utilization of energy performance and the payback period of the dryer. The detailed exergy, and environmental study of a single solar dryer operating in both modes (mixed/indirect) for drying of *Garcinia pedunculata* with and without storage is explored in this chapter. Moreover, the distinguishing characteristic of this dryer is its ability to transform the drying cabinet into different modes effortlessly by adjusting the walls on all four sides of the cabinet. Therefore, this comparative study provides the strengths and weaknesses of each mode, leading to the selection of the most appropriate model. This chapter calculates the exergy in, out, loss and efficiency for SAC and solar dryer (indirect/mixed-mode) with and without storage, and estimates the environmental parameters for the four modes. Based on the same working principle and experimental procedure on the same dryer mentioned in Chapter 4, experiments were performed on the month of April, 2022 and a new set of data was analyzed. The four combinations considered were indirect-mode solar dryer without storage (ID-WOS), mixed-mode solar dryer without storage (MX-WOS), indirect-mode solar dryer with storage (ID-WS), and mixed-mode solar dryer with storage (MX-WS). The feature of this dryer that sets it apart is its capability to convert the drying cabinet into various modes simply by sliding the walls of the four sides of the cabinet. Figure 5.1 gives the layout of the experimental setup.

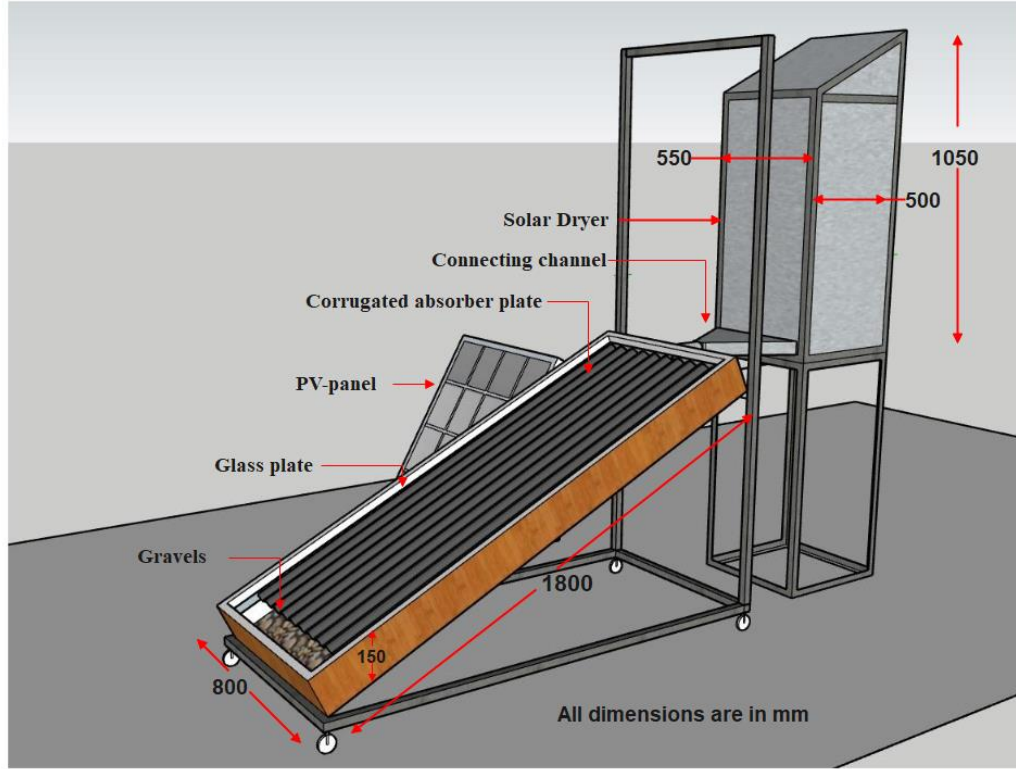


Figure 5.1 Layout of the experimental setup.

5.1 Uncertainty Analysis

Several variables can affect measurements, including calibration, the environment, reading, and others. Eq. (3.1) gives the uncertainty in the result. The uncertainties of moisture loss (weight), temperature, air velocity, solar radiation, $\eta_{Ex,SAC}$ and $\eta_{Ex,dc}$ were ± 0.01 (g), ± 0.1 ($^{\circ}\text{C}$), ± 0.01 (ms^{-1}), ± 1 (Wm^{-2}), ± 1.84 (%) and ± 3.18 (%), respectively.

5.2 Drying Analysis

In the experiments, the samples were weighed periodically with a one-hour interval until their weight remained unchanged, to determine the MC. Eq. (5.1) gives the MC of GP on a wet basis during the drying experiments [132].

$$MC_{GP} = \frac{m_i - m_j}{m_i} \quad (5.1)$$

5.3 Exergy Analysis

Exergy is defined as the maximum work obtained from a system when it interacts with the dead state at equilibrium [19]. In this study, the exergy of the air inlet and outlet to the dryer is evaluated by using Eq. (5.2):

$$\dot{E}x = \dot{m}_a \left[C_{pa}(T - T_\infty) - T_\infty \left\{ C_{pa} \ln \left(\frac{T}{T_\infty} \right) - R \ln \left(\frac{P}{P_\infty} \right) \right\} \right] \quad (5.2)$$

The change in pressure between the inlet and outlet of the dryer of the system is negligible.

The air is assumed as an ideal gas. Therefore Eq. (5.2) becomes Eq.(5.3) [15]:

$$\dot{E}x = \dot{m}_a c_{pa} \left[(T - T_\infty) - T_\infty \ln \left(\frac{T}{T_\infty} \right) \right] \quad (5.3)$$

5.3.1 Exergy analysis of SAC

The exergy balance for SAC is given by Eq. (5.4) [149]:

$$\sum \dot{E}x_{in,SAH} - \sum \dot{E}x_{out,SAH} = \sum \dot{E}x_{l,SAH} \quad (5.4)$$

where $\dot{E}x_{in,SAH}$, $\dot{E}x_{out,SAH}$ and $\dot{E}x_{l,SAH}$ are exergy inflow, outflow, and loss of SAC respectively.

The exergy related to the solar radiation on the SAC is given by Eq. (5.5) [135]

$$\dot{E}x_{in,SAH} = \left[1 - \frac{T_\infty}{T_{sun}} \right] H_{in,abs} \quad (5.5)$$

where T_{sun} is the apparent temperature of the sun (6000 K) [115,150].

The amount of solar radiation falling on the absorber plate is given by Eq. (5.6) [135]

$$\dot{H}_{in,abs} = \alpha \tau I A_{SAH} \quad (5.6)$$

Exergy outflow of wavy SAC is given as Eq. (5.7) [151]

$$\dot{E}x_{out,SAH} = \dot{m}_a c_{pa} \left[(T_{out,c} - T_{in,c}) - T_\infty \ln \left(\frac{T_{out,c}}{T_{in,c}} \right) \right] \quad (5.7)$$

Exergy loss of wavy SAC is the difference between the exergy inflow and exergy outflow and is given by Eq. (5.8)

$$\dot{E}x_{l,SAH} = l = T_\infty S_{gen} = \left[1 - \frac{T_\infty}{T_{sun}} \right] H_{in,abs} - \dot{m}_a c_{pa} \left[(T_{out,c} - T_{in,c}) - T_\infty \ln \left(\frac{T_{out,c}}{T_{in,c}} \right) \right] \quad (5.8)$$

The exergy efficiency of wavy SAC is given by Eq. (5.9) [19,152]

$$\eta_{Ex,SAH} = \frac{\dot{E}x_{out,SAH}}{\dot{E}x_{in,SAH}} = 1 - \frac{\dot{E}x_{l,SAH}}{\dot{E}x_{in,SAH}} \quad (5.9)$$

5.3.2 Exergy analysis of the drying chamber

The exergy inflow is calculated using Eq. (5.10) [15]

$$\sum \dot{E}x_{in,dc} = \dot{m}_a c_{pa} \left[(T_{in,dc} - T_\infty) - T_\infty \ln \left(\frac{T_{in,dc}}{T_\infty} \right) \right] \quad (5.10)$$

The exergy outflow calculated is given as Eq. (5.11)

$$\sum \dot{E}x_{out,dc} = \dot{m}_a c_{pa} \left[(T_{out,dc} - T_\infty) - T_\infty \ln \left(\frac{T_{out,dc}}{T_\infty} \right) \right] \quad (5.11)$$

The subtraction between exergy inflow and exergy outflow is the exergy loss and is given by Eq. (5.12) [153]

$$\sum \dot{E}x_{in,dc} - \sum \dot{E}x_{out,dc} = \sum \dot{E}x_{l,dc} \quad (5.12)$$

where $\dot{E}x_{in,dc}$, $\dot{E}x_{out,dc}$ and $\dot{E}x_{l,dc}$ are exergy inflow, outflow, and loss of the drying chamber respectively.

The exergy efficiency of the drying chamber is calculated by Eq. (5.13) [135].

$$\eta_{Ex,dc} = \frac{\dot{E}x_{out,dc}}{\dot{E}x_{in,dc}} \quad (5.13)$$

5.4 Mass shrinkage ratio

Drying induces structural alterations due to the loss of weight, and among these changes, the most significant variation observed in the crop is represented by the mass shrinkage ratio. The mass shrinkage ratio (SR) given by Eq. (5.14) [52]

$$SR = \frac{m_{t,P}}{m_{i,P}} \quad (5.14)$$

5.5 Environmental Analysis

5.5.1 Energy payback period (EPPD)

The term EPPD in years refers to describe the duration needed to pay back the energy used or spent throughout the manufacturing of the raw materials used for the fabrication of the system and is given by [115]

$$EPPD = \frac{E_{em}(kWh)}{E_{aeo}(kWh/yr)} \quad (5.15)$$

where E_{em} is the embodied energy and E_{aeo} is the annual energy output that is given by Eq (5.16) [154].

$$E_{aeo} = E_{dto} \times N_{sd} \quad (5.16)$$

where E_{dto} given by Eq. (5.17) is the daily thermal output and N_{sd} is the total number of sunshine days in a year and is approximately considered as 250 days [110].

$$E_{dto} = \frac{m_w \times Q_L}{3.6 \times 10^6} \quad (5.17)$$

5.5.2 Carbon-dioxide (CO₂) emission

The amount of average CO₂ emitted in a power plant run by coal is 0.982 kg of CO₂/kWh of the generated electricity [136]. The CO₂ emitted each year is calculated by Eq. (5.18)

$$\text{CO}_2 \text{ emission each year} = \frac{0.98E_{em}}{L_{dry}} \quad (5.18)$$

where L_{dry} is the life span of the dryer is considered as 4, 8, 12, 16, and 20 years.

If domestic losses (20 %) and transmission losses (40 %) are taken into account Eq.(5.18) becomes Eq. (5.19) [110]

$$\text{CO}_2 \text{ emission each year} = \frac{E_{em}}{L_{dry}} \times \frac{1}{1 - L_{da}} \times \frac{1}{1 - L_{tm}} \times 0.98 \text{ kg/year} \quad (5.19)$$

where L_{da} and L_{tm} is the domestic and transmission losses, respectively.

Then Eq. (5.19) becomes Eq. (5.20) [116]

$$\text{CO}_2 \text{ emission each year} = \frac{E_{em}}{L_{dry}} \times 2.042 \text{ kg} \quad (5.20)$$

5.5.3 CO₂ mitigation and Carbon Credit earned (CCE)

CO₂ mitigation of the dryer is estimated using Eq. (5.21) [116]

$$\text{CO}_2 \text{ mitigation} = (E_{aeo}L_{dry} - E_{em}) \times 2.042 \quad (5.21)$$

CCE is calculated using Eq. (5.22)

$$CCE = \text{Net CO}_2 \text{ mitigation} \times \text{Price per ton of the system} \quad (5.22)$$

5.6 Results and discussion

The experiments were performed on days of clear sky in April 2022. The experiments for ID-WOS and MX-WOS were performed from 9:30 h to 16:30 h and from 9:30 h to 18:30 h for ID-WS and MX-WS at a mass flow rate of 0.02 kg/s. Due to variation of solar radiation over the day, therefore data has been collected at different instants within the drying system and the average is taken. The average mass flow rate was approximately reported as 0.02 kg/s. Moreover, the drying rate consistently decreased as drying time progressed as seen in Figure 4.15 and Figure 4.16. This verifies the absence of a constant-rate drying in these curves, indicating that all drying activities take place within the falling-rate drying period. Throughout this phase, diffusion mechanisms primarily governed the drying process. These findings correspond with those reported in existing literature [78,80]. The initial MC of GP, was calculated with the help of the hot-oven method was 87.2 % (w.b.). The final MC was reduced to 12.8 % (w.b.) for ID-WOS in 30 h, for MX-WOS in 25 h, for ID-WS in 28 h, and for MX-WS in 8 h. The hourly change of ambient temperature, SAC's in and out temperatures, and solar radiation without SHS are presented in Figure 5.2, and with SHS is illustrated in Figure 5.3. On Day 1, Day 2, Day 3, Day 4, Day 5, Day 6, and Day 7, the maximum solar radiation was recorded as 911, 920, 915, 924, 912, 921, and 925 W/m², respectively at 11:30 h. Corresponding maximum ambient temperatures on these days were 34.5 °C, 34.8 °C, 34.6 °C, 34.9 °C, 34.2 °C, 34.7 °C, 34.9 °C, respectively. The average inlet temperatures were 34.9 °C, 35.3 °C, 35.4 °C, 35.5 °C, 35.2 °C, 35.6 °C and 35.7 °C, respectively for Day 1 to Day 7. The maximum outlet temperatures were 73.4 °C, 74.3 °C, 74.4 °C, 74.8 °C, 73.5 °C, 74.1 °C, and 75.2 °C, respectively for Day 1 to Day 7. The minimum inlet and outlet temperatures of SAC were recorded at 16:30 h on the days without SHS and at 18:30 h on days with storage. During the lower solar radiation period (16:30-18:30 h), the output temperature of the SAC with SHS was (7.6-14.3) °C higher than the ambient temperature. This is because the gravels-bed provided inside the SAC during the experiment with SHS stored the heat during the initial h and released the heat during the latter half of the day. This helps to extend the period of drying. It could be observed that even after solar radiation decreased subsequently, the SHS aided the absorber plate to maintain the enhanced temperature.

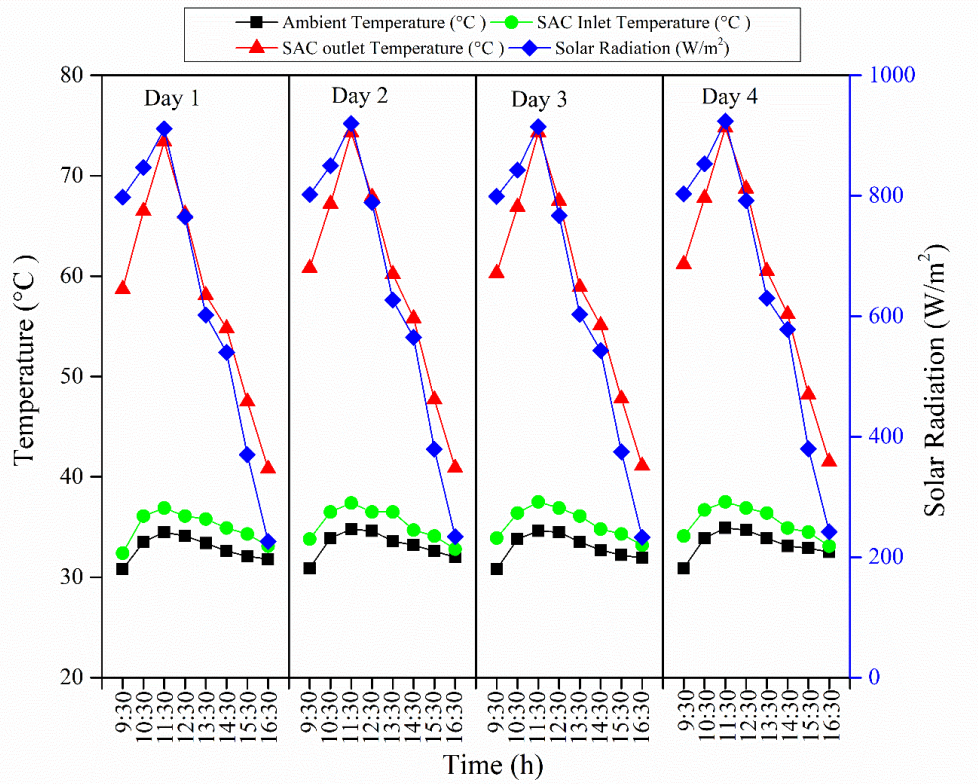


Figure 5.2 Variations of temperatures and solar radiation with time during ID-WOS and MX-WOS.

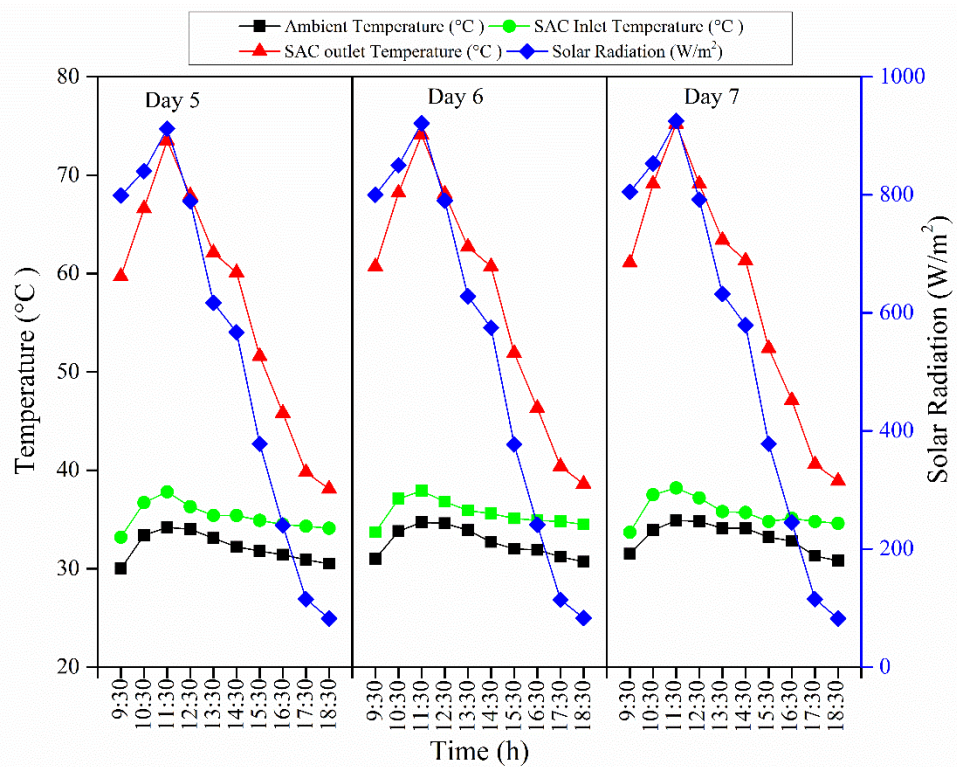


Figure 5.3 Variations of temperatures and solar radiation with time during ID-WS and MX-WS.

The inlet and outlet temperatures of ID-WOS and MX-WOS are plotted in Figure 5.4. The inlet temperature ranged between 42.2 °C-64.1 °C for ID-WOS and 44.7 °C-71.4 °C for MX-WOS. The outlet temperature varied between 38.9 °C-54.8 °C for ID-WOS and 43.2 °C-63.8 °C for MX-WOS. Figure 5.5 gives the dryer inlet and outlet temperature for ID-WS and MX-WS. The inlet temperature varied between 43.2 °C-63.1 °C for ID-WS and 52.4 °C-73.6 °C for MX-WS. The outlet temperature varied between 40.5 °C-57.2 °C for ID-WS and 51.1 °C- 60.2 °C for MX-WS. The temperature reaches the maximum at 11:30 h. It may be observed that during the latter part of the day, as the intensity of radiation decreases, the addition of the gravel as storage has sufficiently provided heat to the dryer.

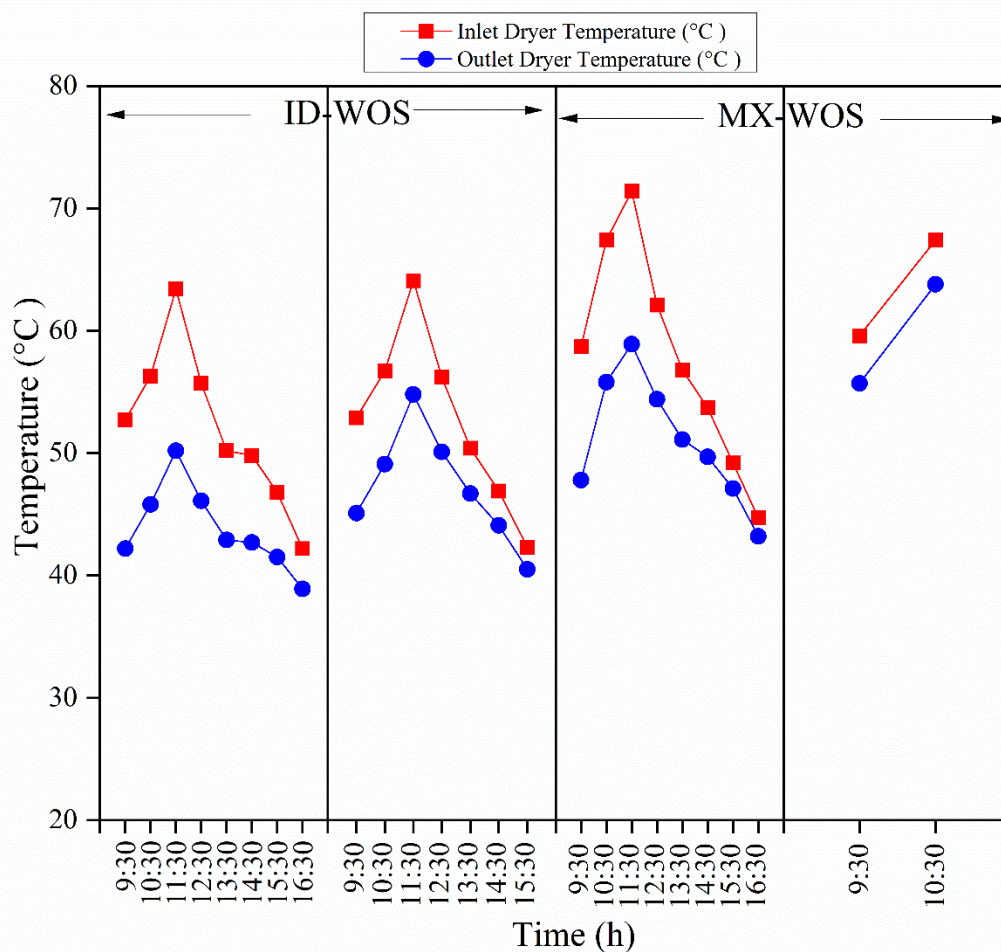


Figure 5.4 Variations of dryer inlet and outlet temperatures with drying time in ID-WOS and MX-WOS.

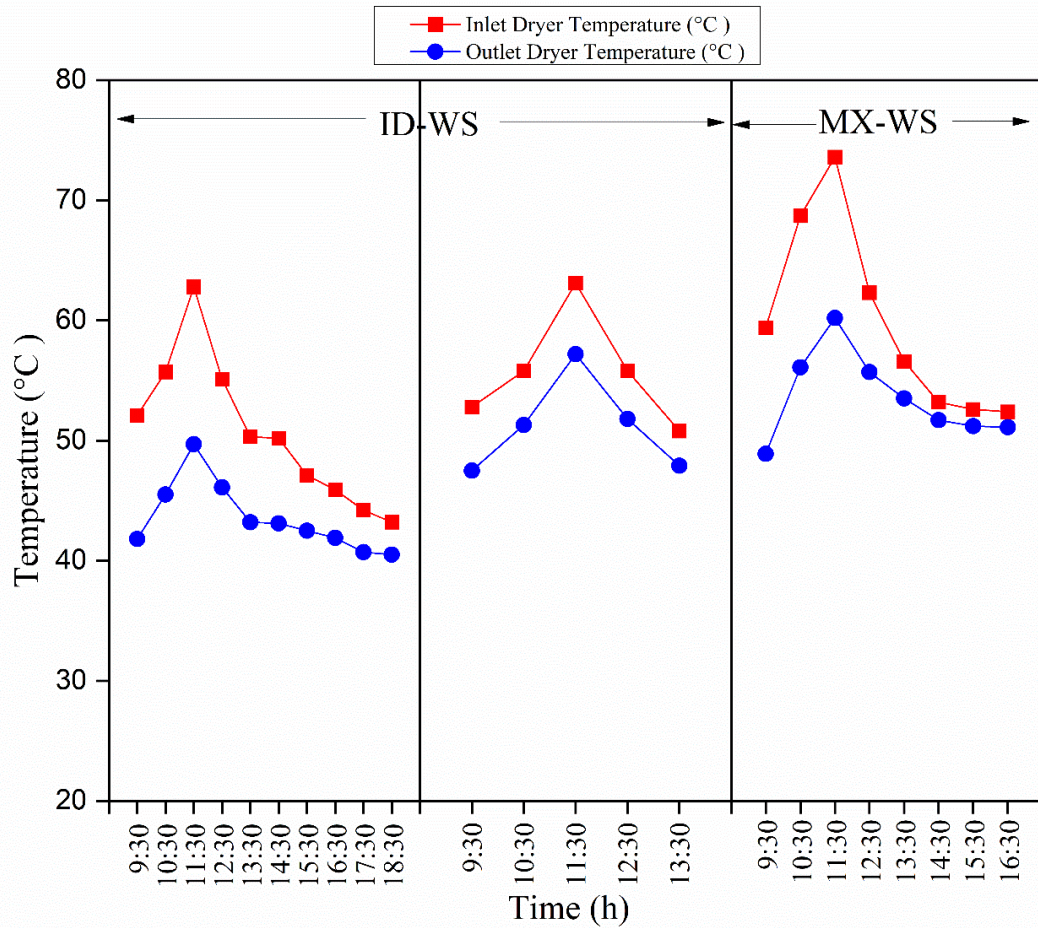


Figure 5.5 Variations of dryer inlet and outlet temperatures with drying time in ID-WS and MX-WS.

5.6.1 Exergy Analysis

The hourly variation of exergy in, out, loss, and efficiency in SAC with time without SHS is plotted in Figure 5.6 and with SHS is plotted in Figure 5.7, respectively. The exergy in was in the range of 261.40-1053.22 W, 270.64-1063.57 W, 269.49-1057.82 W, 279.87-1068.17 W, respectively from Day 1 to 4 and in the range from 94.86-1054.43 W, 96.01-1064.75 W, and 94.86-1069.33 W from Day 5 to Day 7. The exergy out varied as 21.61-263.12 W, 21.37-268.02 W, 22.46-270.69 W, and 21.62-271.94 W, respectively from Day 1 to Day 4 and 12.71-266.91 W, 13.44-266.44 W, 14.25-275.23 W, respectively from Day 5 to Day 7. It can be observed that the minimum exergy in and out for the days with storage is lower than the days without storage. This is because the minimum occurred at 18:30 h for the days with storage corresponding to solar radiation of 82-83 W and at 16:30 h for the days without storage for solar radiation of 226-242 W. The exergy loss varied in the range of 239.79-790.09 W, 249.27-795.54 W, 247.02-787.13 W and 258.25-796.23 W, respectively

from Day 1 to Day 4 and 82.15-787.51 W, 82.57-798.31 W, 80.60-794.10 W, respectively for Day 5 to Day 7. The exergy in, out, and loss followed the same behaviour. From the figure, it could be implied that the solar radiation and the air temperature of the SAC in and out influence the exergy loss. The exergy efficiency varied in the range 8.26-24.98 %, 7.89-25.20 %, 8.33-25.58 % and 7.72-25.46 %, respectively from Day 1 to Day 4 and 13.39-25.31 %, 14.00-25.02 %, 15.02-25.73 %, respectively for Day 5 to Day 7.

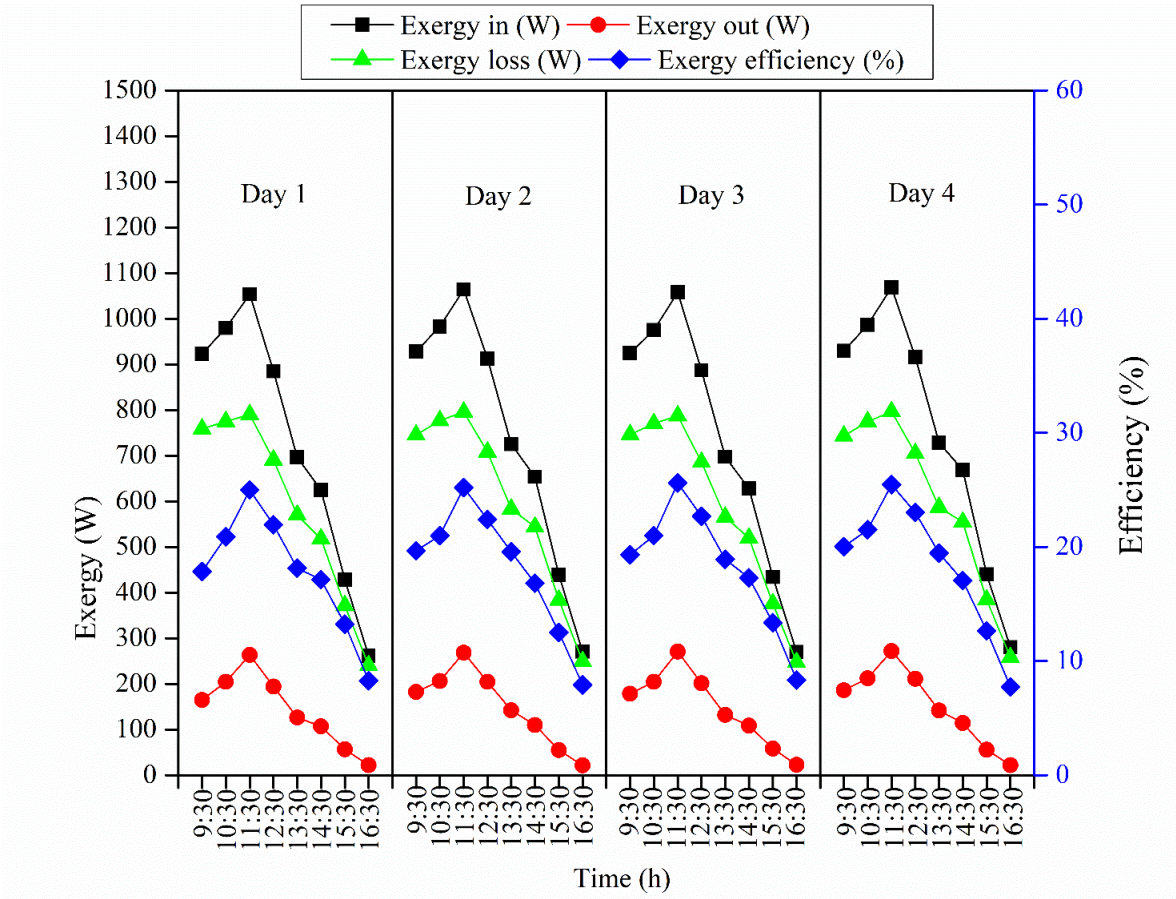


Figure 5.6 Variations of exergy in, out, loss, and efficiency of SAC with drying time during ID-WOS and MX-WOS.

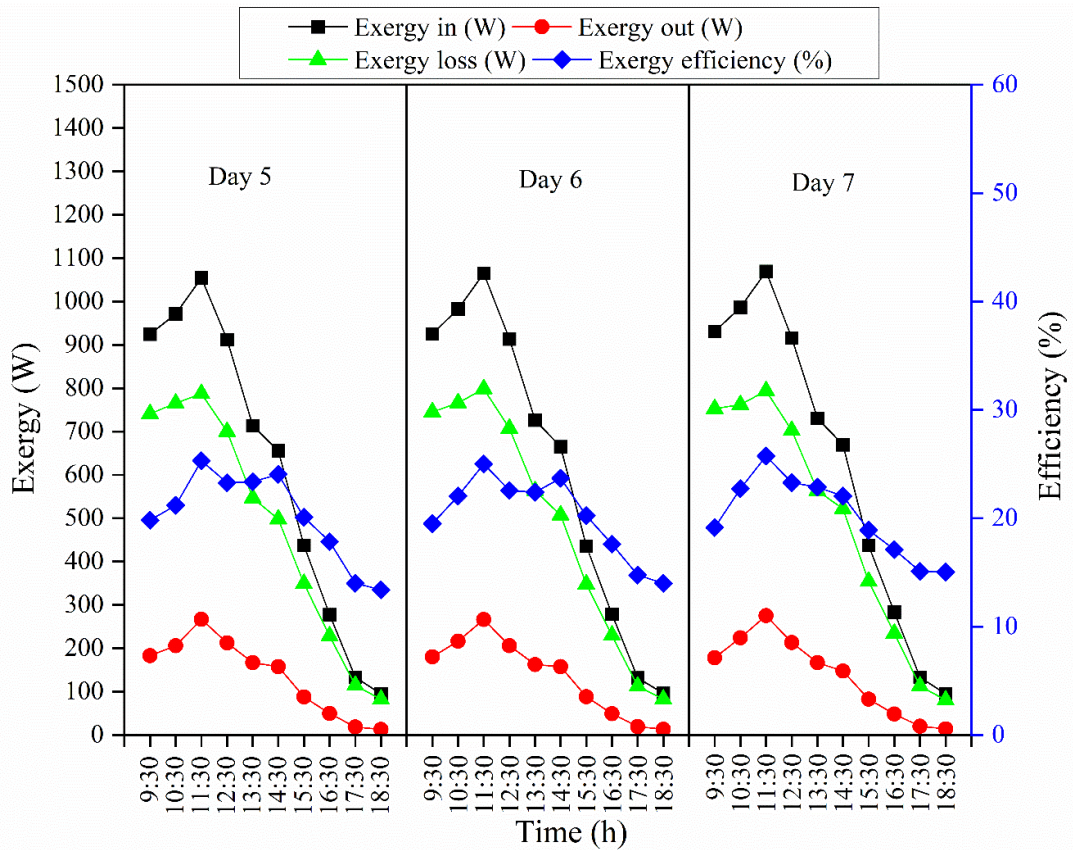


Figure 5.7 Variations of exergy in, out, loss, and efficiency of SAC with drying time during ID-WS and MX-WS.

The variation of exergy in, out, loss, and efficiency in the dryer with time without SHS is plotted in Figure 5.8 and with SHS is plotted in Figure 5.9, respectively. From the figure, it could be inferred that during the initial hour of the day (till 11:30 h), the exergy in, out and loss increased and it subsequently, decreased during the latter half of the day for all four cases. The average exergy inflow was calculated as 88.35 W, 147.78 W, 90.45 W and 144.29 W for ID-WOS, MX-WOS, ID-WS and MX-WS, respectively while average exergy outflows were 39.38 W, 92.08 W, 46.39 W, and 87.98 W, respectively. The exergy in, out and loss is more in a mixed mode than in an indirect mode. It is because the temperature of the air inside the drying chamber during mixed mode receives radiation both from the SAC and the walls of the dryer. The exergy efficiencies were in the range of 31.74-68.35 %, 43.09-82.95 %, 33.37-71.53 %, and 44.78-88.55 %, respectively for ID-WOS, MX-WOS, ID-WS and MX-WS. With the passing hour of the day, the exergy efficiency gradually rises. Since the exergy outflow moves closer to the exergy intake of the drying chamber, it demonstrates that the exergy efficiency rises as the drying process advances. Moreover, the final day of the dehydration stage was when exergy efficiency was recorded to be at its

maximum. It occurred because there was little moisture left in the product when the dehydration process came to a close and the product uses less energy during the last stage of drying. A similar observation was made in Ref. [15,102]. Further, the average exergy efficiency of the solar dryer in ID-WOS, MX-WOS, ID-WS and MX-WS is found to be 47.08, 65.10, 52.46 and 68.07 %, respectively. It is worth noting that the average exergy efficiency of solar dryer developed in the present study in MX-WS is 8.05 % (ghost chilli pepper) and 44.83 % (ginger) higher than the solar dryer studied in [15] and 4.40 % (pear slices) higher than the solar dryer studied in [102].

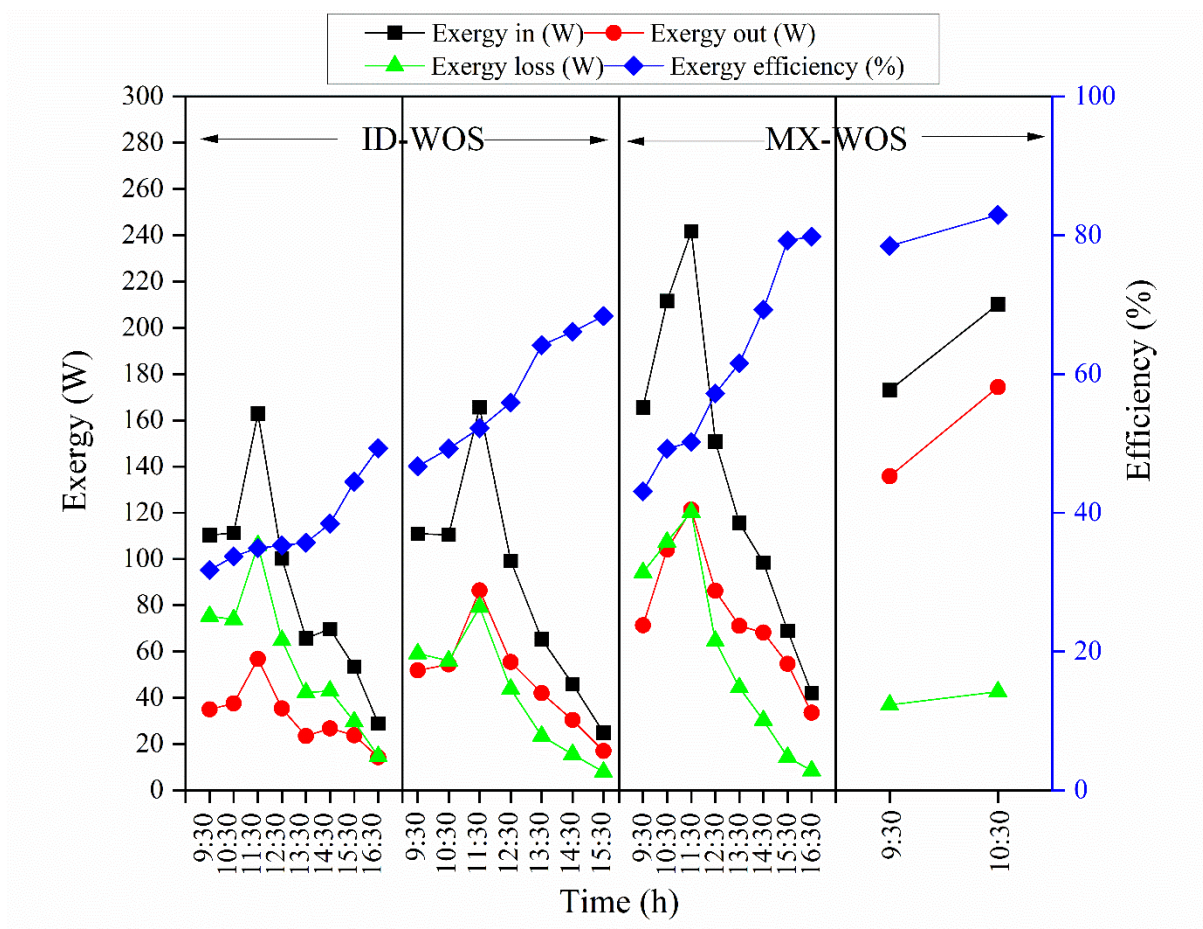


Figure 5.8 Variations of exergy in, out, loss and efficiency of the dryer with drying time during ID-WOS and MX-WOS.

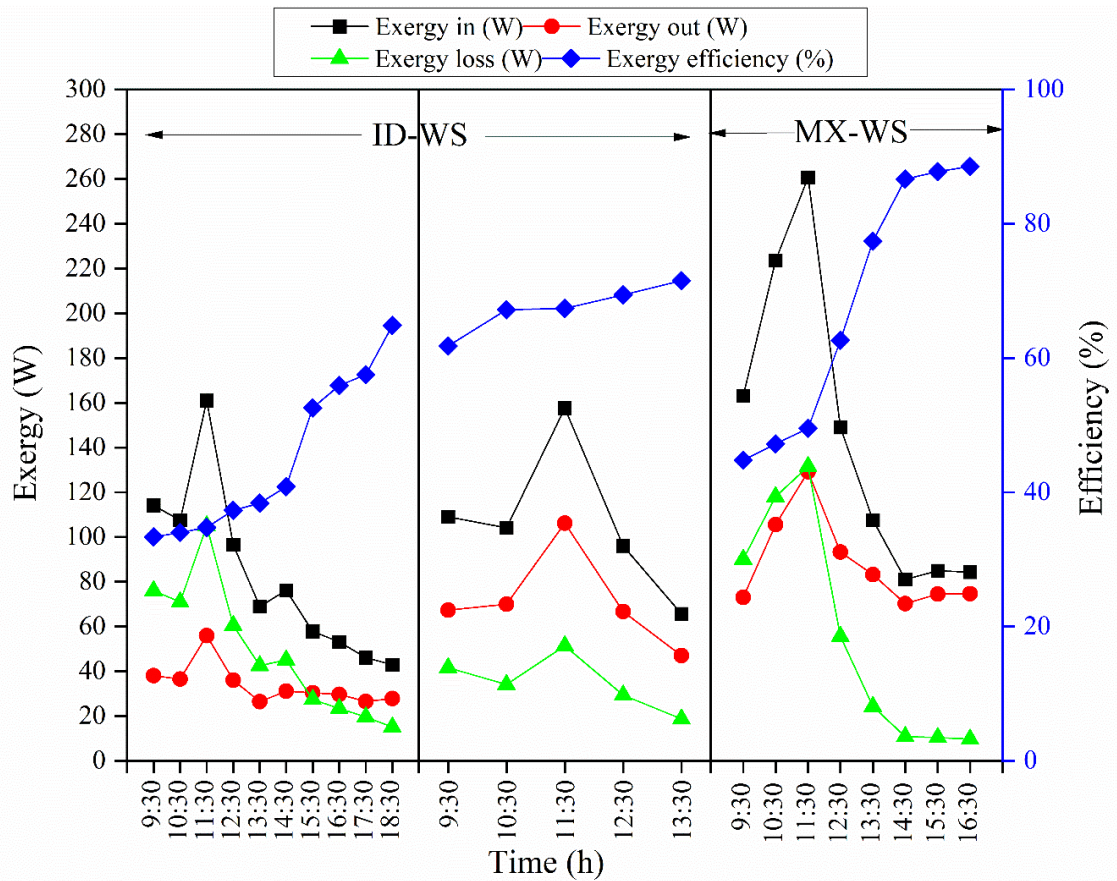


Figure 5.9 Variations of exergy in, out, loss and efficiency of the dryer with drying time during ID-WS and MX-WS.

5.6.2 Mass shrinkage ratio

The mass shrinkage ratio (SR) of the dried *Garcinia pedunculata* is derived using Eq. (5.14). The SR and exergy efficiency for ID-WOS, MX-WOS, ID-WS, and MX-WS are plotted in the Figure 5.10 for the initial drying day. At the initial stage, when the MC of the GP is high, the exergy efficiency tends to be low due to the considerable energy input needed for moisture removal. However, as the day progresses, the rate of shrinkage slows down as the moisture content decreases, leading to an increase in exergy efficiency. This trend occurs because less energy is needed to remove moisture from the material as its moisture content decreases. Further, notable shrinkage of *Garcinia pedunculata* in MX-WS was observed when compared to ID-WOS.

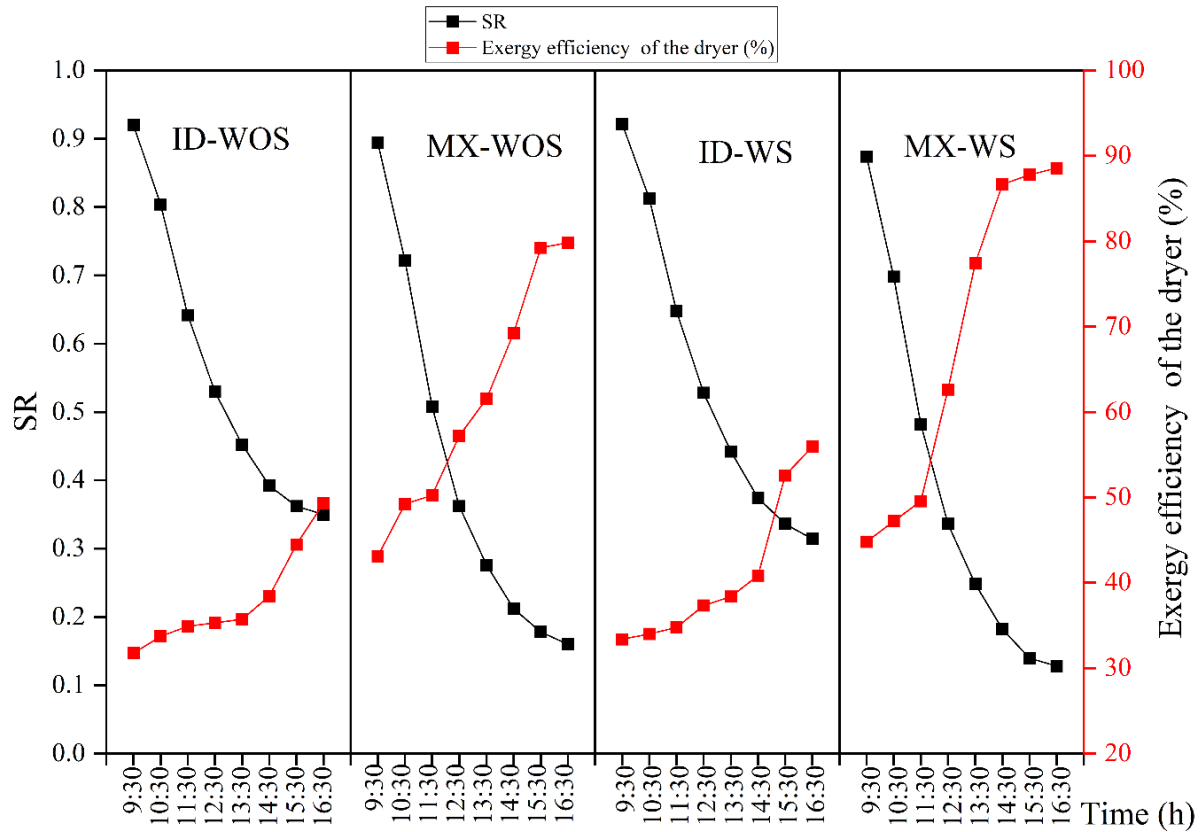


Figure 5.10 Variations of SR and Exergy efficiency of the dryer with time for ID-WOS, MX-WOS, ID-WS and MX-WS

5.6.3 Environment Analysis

Environmental research was carried out on the four modes of the dryer to determine the effect on the environment when constructing and using the dryer. The total energy consumed to manufacture of a product is termed the embodied energy and is given in Table 5.1 and Table 5.2 for the drying system without and with storage, respectively. It can be observed that for the drying systems without storage, the total mass was less than the drying systems with storage. However, this entirely did not affect the embodied energy as the energy density of gravels is less. The embodied energy for ID-WOS, MX-WOS, ID-WS, and MX-WS were 1011.67, 1109.24, 1014.73, and 1112.30 kWh, respectively.

Table 5.1 Mass and Embodied Energy of the different components of dryer without storage.

Sl. No.	Parts	Materials	Energy density (kWh/kg) [110,136]	Mass (kg)		Embodied Energy (kWh)	
				ID-WOS	MX-WOS	ID-WOS	MX-WOS
1	Absorber plate	Al	55.28	3.80	3.80	210.06	210.06
2	Glass cover	Glass	7.28	3.60	3.60	26.21	26.21
3	Packed Bed	Gravels	0.03	0.00	0.00	0.00	0.00
4	Coating	Black paint	25.11	0.50	0.50	12.56	12.56
5	Frames	Mild steel	8.89	29.70	29.70	264.03	264.03
6	Walls	Plywood	0.66	6.30	0.00	4.16	0.00
7	Walls	Steel	8.89	7.02	0.00	62.41	0.00
8	Walls	Acrylic sheet	28.30	0.00	5.80	0.00	164.14
9	Fittings	Mild steel	8.89	1.00	1.00	8.89	8.89
10	Trays	Mild steel	8.89	8.25	8.25	73.34	73.34
11	Cu wire	Copper	19.61	0.50	0.50	9.81	9.81
12	Piping	PVC	19.39	0.50	0.50	9.70	9.70
13	Insulation	Cotton	15.28	1.50	1.50	22.92	22.92
14	DC fan	Plastic	19.40	0.12	0.12	2.33	2.33
15	PV modules	Solar cell (kWh/m ²)	1130.60	0.27 m ²	0.27 m ²	305.26	305.26
Total				63.06	55.54	1011.67	1109.24

Table 5.2 Mass and Embodied Energy of the different components of dryer with storage.

Sl. No.	Parts	Materials	Energy density (kWh/kg) [110,136]	Mass (kg)		Embodied Energy (kWh)	
				ID-WS	MX-WS	ID-WS	MX-WS

1	Absorber plate	Al	55.28	3.80	3.80	210.06	210.06
2	Glass cover	Glass	7.28	3.60	3.60	26.21	26.21
3	Packed Bed	Gravels	0.03	110.00	110.00	3.06	3.06
4	Coating	Black paint	25.11	0.50	0.50	12.56	12.56
5	Frames	Mild steel	8.89	29.70	29.70	264.03	264.03
6	Walls	Plywood	0.66	6.30	0.00	4.16	0.00
7	Walls	Steel	8.89	7.02	0.00	62.41	0.00
8	Walls	Acrylic sheet	28.30	0.00	5.80	0.00	164.14
9	Fittings	Mild steel	8.89	1.00	1.00	8.89	8.89
10	Trays	Mild steel	8.89	8.25	8.25	73.34	73.34
11	Cu wire	Copper	19.61	0.50	0.50	9.81	9.81
12	Piping	PVC	19.39	0.50	0.50	9.70	9.70
13	Insulation	Cotton	15.28	1.50	1.50	22.92	22.92
14	DC fan	Plastic	19.40	0.12	0.12	2.33	2.33
15	PV modules	Solar cell (kWh/m ²)	1130.60	0.27 m ²	0.27 m ²	305.26	305.26
	Total			173.06	165.54	1014.73	1112.30

Energy payback period (EPPD)

The EPPD was estimated to be 1.47, 1.61, 1.48, and 1.62 years, respectively for ID-WOS, MX-WOS, ID-WS, and MX-WS. Comparing this duration to the lifetime (20 years) of the developed solar dryer, it is significantly shorter. Given that the solar dryer has a 20-years life expectancy, the CO₂ emission, CO₂ mitigation, Carbon credit (5 \$ base) and Carbon credit (20 \$ base) for a lifetime of 4, 8, 12,16 and 20 years are given in Table 5.3.

The findings of the current study are consistent with those of [110], whose study demonstrated values of energy payback, CO₂ mitigation, and carbon credit as 2.21 years, 33.52 tons, and ranging from \$144.772 to \$579.087, respectively, over a 35-year lifespan. Chauhan *et al.* [116] studied a solar dryer integrated with a solar air heater, and assessed its

energy efficiency. The energy payback time was determined to be 1.68 years under natural mode and 2.35 years under forced mode, with net CO₂ mitigation values of 33.04 and 36.34 tons, respectively. The energy analysis demonstrated that the dryer was both cost-effective and environmentally friendly, making it a recommended choice for the drying of agricultural goods.

Table 5.3 CO₂ emission, CO₂ mitigation and Carbon credit of the dryer.

Type		Life of the dryer (years)				
		4	8	12	16	20
ID-WOS	Yearly CO ₂ emission in kg	627.23	313.62	209.08	156.81	125.45
	Yearly CO ₂ mitigation in tons	4.31	11.13	17.95	24.77	31.59
	Carbon credit in \$ (5 \$ base)	21.56	55.66	89.76	123.86	157.96
	Carbon credit in \$ (20 \$ base)	86.22	222.62	359.02	495.42	631.82
MX-WOS	Yearly CO ₂ emission in kg	687.73	343.87	229.24	171.93	137.55
	Yearly CO ₂ mitigation in tons	4.07	10.89	17.71	24.53	31.35
	Carbon credit in \$ (5 \$ base)	20.35	54.45	88.55	122.65	156.75
	Carbon credit in \$ (20 \$ base)	81.38	217.78	354.18	490.58	626.98
ID-WS	Yearly CO ₂ emission in kg	629.13	314.57	209.71	157.28	125.83
	Yearly CO ₂ mitigation in tons	4.30	11.12	17.94	24.76	31.58
	Carbon credit in \$ (5 \$ base)	21.52	55.62	89.72	123.82	157.92
	Carbon credit in \$ (20 \$ base)	86.07	222.47	358.87	495.27	631.67
MX-WS	Yearly CO ₂ emission in kg	689.63	344.81	229.88	172.41	137.93
	Yearly CO ₂ mitigation in tons	4.06	10.88	17.70	24.52	31.34
	Carbon credit in \$ (5 \$ base)	20.31	54.41	88.51	122.61	156.71
	Carbon credit in \$ (20 \$ base)	81.23	217.63	354.03	490.43	626.83

5.7 Summary

Another set of experiments were performed to analyze the exergy and environmental impact of the solar dryer. The four combinations considered were indirect-mode solar dryer without storage (ID-WOS), mixed-mode solar dryer without storage (MX-WOS), indirect-mode solar dryer with storage (ID-WS), and mixed-mode solar dryer with storage (MX-WS). The final MC was decreased to 12.8 % (w.b.) for ID-WOS in 30 h, for MX-WOS in 25 h, for ID-WS in 28 h and for MX-WS in 8 h from an initial of 87.2 % (w.b.). The following conclusion was inferred:

- It was observed that SAC with SHS was more effective than SAC without SHS at the same mass flow rate. After 12:30 h, the efficiency of the SAC with storage increased while the efficiency of the one without storage decreased. During the first half of the day, the efficiencies of both cases (without and with SHS) were similar.
- Exergy studies can assist in identifying the true potential of solar systems. Due to exergy losses from various collector components, the wavy collector had relatively low exergy efficiencies when compared to their thermal efficiencies. In this experiment, it was observed that the dryer had high exergetic efficiencies toward the end of the drying intervals.
- The average exergy efficiency of the drying chamber in ID-WOS, MX-WOS, ID-WS, and MX-WS were calculated as 47.08 %, 65.10 %, 52.46 % and 68.07 %, respectively.
- During the 20 years life-span of the dryer, the CO₂ emission were 125.45 kg, 137.55 kg, 125.83 kg and 137.93 kg respectively for ID-WOS, MX-WOS, ID-WS, and MX-WS and the corresponding CO₂ mitigation were 31.59 tons, 31.35 tons, 31.58 tons and 31.34 tons, respectively.
- The total embodied energy of the mixed-mode was higher than the indirect-mode leading to an increase in the payback period. But the use of gravels as storage did not significantly increase the CO₂ emission, CO₂ mitigation and carbon credit as the energy density of gravels is less.
- For ID-WOS, MX-WOS, ID-WS, and MX-WS, the anticipated EPPD were 1.47, 1.61, 1.48, and 1.62 years, respectively. According to this study, the performance of MX-WS was better than the other three configurations in all its factors.